NORDIC STEEL 2024
The 15th Nordic Steel Construction Conference,
June 26–28, 2024, Luleå, Sweden

Flexural buckling of mild and high-strength steel hot-rolled sections

Improvement proposal of the flexural buckling design rules

Loris Saufnay*[,a], Jean-François Demonceau[a]

[a]Urban and Environmental Engineering (UEE) department, University of Liège, Liège, Belgium
loris.saufnay@uliege.be, jfdemonceau@uliege.be

ABSTRACT

The determination of the bearing capacity of a member under compression, presenting an initial out-of-straightness and residual stresses resulting from the production process, requires dealing with a stability problem governed by the geometry of the member and the mechanical properties of its constitutive material. Amongst these, the yield strength plays a key role. Indeed, it has a direct impact on the plastic resistance of the member but, also, the detrimental effect of initial imperfections decreases as the yield strength increases. The effect of these initial imperfections is considered by an imperfection factor α in the design recommendations provided in EN1993-1-1. However, the current and new upcoming versions of this norm give a step evolution of this imperfection as a function of yield strength by only distinguishing grades smaller or higher than S460. The present paper aims to briefly summarise the existing studies on this topic, to assess the recommendations of both versions of EN1993-1-1, and to propose a continuous form of the imperfection factor for hot-rolled sections for existing grades up to S500 and even higher grades as a prospective study. The validity of the proposed imperfection factor will be finally assessed for H-shaped cross-sections with height-to-width ratios h/b>1.2 and flange thicknesses $t_f \leq$ 40mm.

Keywords: High-strength steels, Flexural buckling, Hot-rolled sections, Finite element simulations,

1 INTRODUCTION

1.1 European buckling curves

According to the design recommendations of Eurocode 3 (1), the resistance of an element subjected to compression is checked using *Eq. (1)*.

$$N_{b,Rd} = \frac{\chi * \beta * A * f_y}{\gamma_{M1}} \geq N_{Ed} \quad (1)$$

where $N_{b,Rd}$ is the design buckling resistance, N_{Ed} the design value of the compression force, χ the reduction factor to account for the risk of flexural buckling, β the reduction factor to account for the risk of local plate buckling, A the cross-sectional area, f_y the yield strength and γ_{M1} the partial safety coefficient for stability problems.

The geometrical and material imperfections are accounted for by the well-known European buckling curves $\chi = f(\bar{\lambda})$ in the design procedures, where $\bar{\lambda}$ is the relative slenderness of the member. These curves allow to predict the characteristic resistance values of members in compression based on more than 1000 experimental tests performed under the auspices of the European Convention for Constructional Steelwork (ECCS) in various European countries in the ’60s (2) and on a theoretical study through which the curves have been derived (3). These studies led to a proposition of buckling curves for which the safety has been assessed by Monte-Carlo simulations (4). Finally, Maquoi and

Rondal derived the current Ayrton-Perry format of the buckling curves (5), which is still used nowadays for design. This formulation is expressed in *Eq. (2)*.

$$\chi = \frac{1}{\phi - \sqrt{\phi^2 - \bar{\lambda}^2}} \text{ with } \phi = 0.5 * (1 + \eta + \bar{\lambda}^2) \text{ where } \eta = \alpha * (\bar{\lambda} - 0.2) \quad (2)$$

with η the imperfection parameter and α the imperfection factor.

This parameter α can take different values according to EN1993-1-1 (1) as listed in *Table 1*.

Table 1. Buckling curve specification according to EN1993-1-1 (1).

Buckling curve	a_0	a	b	c	d
Imperfection factor	0.13	0.21	0.34	0.49	0.76

The buckling curve selection depends on the cross-section shape, the buckling axis, the cross-section height-to-width *h*/*b* ratio, the flange thickness t_f and the production process that influences the residual stress pattern, and therefore the buckling resistance of the member.

1.2 Literature review about the yield strength impact on buckling resistance

The buckling curves were originally established based on a fictitious material characterized by an elastic limit $f_y = 255$ MPa. Indeed, the experimental campaign was realized in the '60s using mild steels with low thickness (below 40mm) while only a few tests were performed on higher steel grades, equivalent to current S275 and S355. It was concluded at that time that the yield strength had little influence on the dimensionless buckling curves, which justifies that they were established for a fixed value of 255 MPa (3).

In opposition to this statement, it was later shown that residual stress distributions do not evolve proportionally with the yield strength, leading to an increase in buckling resistances for higher grades as the local yielding is delayed. For hot-rolled cross-sections, the residual stresses effectively depend on the geometrical cross-section properties and the cooling rate during the production process and are definitively not proportional to the yield strength (6) as confirmed by experimental investigations (7). In fact, the residual stress-to-yield strength ratio decreases when the yield strength increases. It could therefore have been decided to define the imperfection factor as a function of the yield strength to consider the beneficial effect of an increasing yield strength on the member buckling resistance. In 1976, the ECCS recommendations (8) allowed a jump of one buckling curve when the yield stress reaches 430 MPa. At that time, Maquoi even established a yield strength-dependent expression for the imperfection factor (9) based on these recommendations, respecting the "jump" between mild and high-strength grades as reported in *Eq. (3)*.

$$\alpha^* = \alpha * \left(\frac{235}{f_y}\right)^{0.8} \quad (3)$$

Maquoi (9) decided to consider S235 as the reference, together with an exponent of 0.8 to respect the jump of one buckling curve preconized in the ECCS recommendations. In this manner, if $\alpha = 0.34$ for S235, which corresponds to curve "b", $\alpha^* = 0.21$ for S430, which corresponds to buckling curve "a". Similarly, if $\alpha = 0.21$ for S235, $\alpha^* = 0.13$ for S430, which corresponds to buckling curve "a_0". However, when $\alpha = 0.49$ for S235, which corresponds to curve "c", $\alpha^* = 0.30$ for S430, which does not correspond to buckling curve "b". This feature was not discussed at that time and considering that this proposal was based on a limited number of experimental tests, it was therefore not implemented in design standards. The research campaign for S460 subsequently led to a beneficial adaptation of the buckling curve selection for this specific grade. So nowadays, only S460 benefits from the reduced influence of the residual stresses for higher yield strength. Indeed, the curves initially established for a yield stress of 255 MPa were considered applicable without modifications for grades from S235 up to S420 while grade S460 got preferential treatment; this is still the case in both Eurocode versions (1,10). In some cases, the buckling curve a_0 is even recommended for S460 whereas this curve was

originally established for sections without any residual stresses (Beer & Schulz 1970) - the subscript 0 meaning “zero residual stresses” - which demonstrates the inconsistency of the currently proposed discrete buckling curves (11).
However, intermediary grades between S235 and S460 may deserve higher buckling curves than the ones currently preconized, what will be demonstrated in the present paper. Indeed, for several years, given the number of experimental and numerical investigations about the structural behaviour of members made of high-strength steels (12–20), some authors (9,13,21–23) have proposed new expressions of the imperfection parameter η (see (2)) in which the influence of the yield strength is explicitly accounted for. The proposed equations for the imperfection parameter are listed by section typologies in *Table 2*.

Table 2. Proposed continuous expressions of the imperfection parameter η found in literature.

Type of sections	Maquoi, 1982	Jönsson & Stan, 2016	Somodi & Kövesdi, 2017	Meng & Gardner, 2020
Hot-rolled (y-y)		$\alpha * (\bar{\lambda}\varepsilon - 0{,}2)$ with; $\varepsilon = \sqrt{\frac{235}{f_y}}$ Class 4 neglected, only for strong axis buckling	/	/
Hot-rolled (z-z)	$\boldsymbol{\alpha^* * (\bar{\lambda} - 0{,}2)}$ $\alpha^* = \alpha * \left(\frac{235}{f_y}\right)^n$ n=0.8, Maquoi, 1982 ; n=1.0, Johansson, 2005 ;	/	/	/
Welded I-sections		/	$\boldsymbol{\alpha^* * (\bar{\lambda} - 0{,}2)}$ $\alpha^* = \alpha * \left(\frac{235}{f_y}\right)^{0.6}$	/
Hot-finished tubes		/	/	$\boldsymbol{\alpha^* * (\bar{\lambda} - 0{,}1)}$ $\alpha^* = 0.24\varepsilon$ for hot-finished $\alpha^* = 0.56\varepsilon$ for cold-formed
Cold-formed tubes		/	$\boldsymbol{\alpha^* * (\bar{\lambda} - 0{,}2)}$ $\alpha^* = \alpha * \left(\frac{235}{f_y}\right)^{0.5}$	

According to *Table 2*, there exist different approaches for considering the influence of the yield strength on the imperfection factor. It has been decided to consider the approach of Maquoi (9) as it enables; (i) to keep the same historical buckling curves for S235, (ii) to keep the length of the plastic plateau as currently defined in design recommendations and (iii) to avoid proposing different specific imperfection factors for each steel grade. The exponent could be different depending on the section typology as demonstrated in several studies by Somodi & Kövesdi (22,23).
In addition, similarly to what was recommended in 1976 for a yield strength of 430 MPa, the new version FprEN1993-1-1(10) recommends a jump of one buckling curve for 460 MPa for all geometry limits and buckling axes in the category of hot-rolled sections. Therefore, considering the same approach as Maquoi did in 1982 (9) makes sense. In this research, the exponent *n* is fixed equal to 0.7, to respect the current imperfection factors for S235 and S460. Indeed, by using this exponent, if $\alpha = 0.21$, $\alpha^* = 0.21$ for S235 and $\alpha^* = 0.13$ for S460. Similarly, if $\alpha = 0.34$, $\alpha^* = 0.34$ for S235 and $\alpha^* = 0.21$ for S460 while there is still a small gap when $\alpha = 0.49$. The validity of this proposal will be evaluated through numerical investigations in this paper.

2 RESEARCH OBJECTIVES AND METHODOLOGY

This paper aims to evaluate the effect of the yield strength on the buckling resistance of columns under compression as well as to propose a new imperfection factor expression to accurately account for the yield strength effect. The pursued methodology consists of calculating buckling resistances based on numerical simulations performed by using the FineLg finite element software developed by the Greisch design office and the University of Liège (24). This software has been used and validated through many studies conducted in the past to model instability phenomena (25–29). The numerical investigations focus on hot-rolled sections in existing grades ranging between S235 and S500, but also in possible future emerging higher grades (up to S690), therefore in the framework of a prospective study. The yield strength f_y of steel grades is considered equal to the recommended values in FprEN1993-1-1 for grades up to S700 depending on the thickness domain, i.e., $t_f \leq 40$mm or 40mm $< t_f \leq 80$mm (10). The HISTAR® trademark steels of ArcelorMittal offer improved yield strengths up to higher flange thickness; for instance, the nominal yield strength is conserved up to 100 mm for HISTAR® 460 (30). However, according to product standards EN10025-2 (31) and EN10025-4 (32), even for flange thicknesses below 40mm, a small decrease in the yield strength is contemplated, the effect of this eventual reduction is also addressed in this paper by considering the yield strength associated with the flange thickness as prescribed in the above-mentioned product standards (*Fig*. 1).

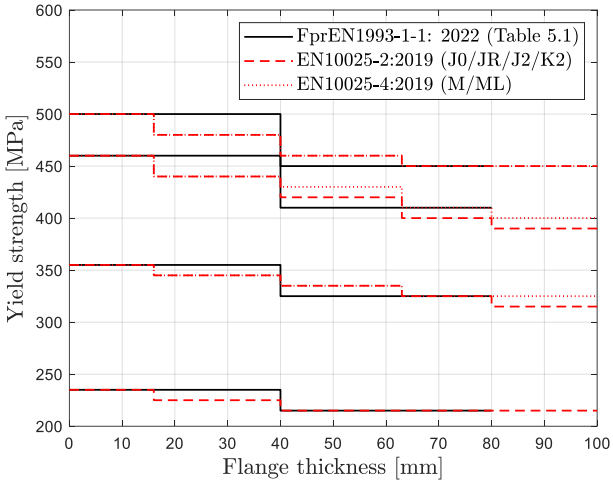

Fig. 1. Evolution of the yield strength depending on the flange thickness.

The validity of the proposed modified imperfection factor, i.e., the Maquoi's formulation (9) with an exponent of 0.7, is evaluated on H-shaped cross-sections with height-to-width ratios h/b>1.2 and flange thicknesses $t_f \leq$ 40mm in this paper for which the benefit in using higher yield strength is expected to be significant. Indeed, higher thicknesses have already been investigated in a previous study in which the negative impact of the yield strength reduction associated to the use of higher thicknesses was observed (33). Moreover, only a few sections exist with thicknesses higher than 100mm for h/b>1.2 (already studied in (33)).

Flexural buckling about both buckling axes is studied and, to simulate a buckling curve, 13 simply supported columns with classes 1-3 cross-sections are modelled corresponding to 13 various reduced slendernesses along the buckling curve; each specimen length corresponding to the targeted reduced slendernesses is obtained using the Eurocode relative slenderness (*Eq. (4)*):

$$\bar{\lambda} = \sqrt{\frac{A * f_y}{N_{cr}}} \rightarrow L = L_{fl} = \frac{i * \pi * \bar{\lambda}}{\sqrt{\frac{f_y}{E}}} \tag{4}$$

Based on failure loads obtained by numerical simulations, the corresponding reduction factor for classes 1-3 cross-sections can be derived as:

$$\chi = \frac{N_{u,GMNIA}}{A_{GMNIA} * f_y} \quad (5)$$

The correspondence between Eurocode and numerical buckling curves is evaluated by calculating the mean value ($\bar{x}$), the standard deviation (COV) and the minimum and maximum values of the ratios between numerical and analytical reduction factors $\left(\frac{\chi_{GMNIA}}{\chi_{EC3}}\right)$. A buckling curve is assumed to be suitable when the mean value is above 1.0, this limit corresponds to the partial safety coefficient for stability design calculations ($\gamma_{M1} = 1.0$). The statistical evaluation and the figures presenting the results of the study have been realized by means of the MATLAB software (34). A summary of the wide numerical campaign, including geometrical properties of the selected cross-sections and the cross-section classification to justify the use of beam finite elements is reported in *Table 3*. Additional numerical simulations for HEM500 were realized considering the yield stress reduction according to product standards EN10025-2 and EN10025-4 (31,32).

Table 3. Geometrical properties and type of finite elements for each selected cross-section.

Limits	Designation	h [mm]	b [mm]	t_w [mm]	t_f [mm]	r [mm]	Class in S460	Class in S690
h/b > 1.2	HEB400	400	300	13.5	24	27	2	3
/ $t_f \leq 40$mm	HEM500	524	306	21	40	27	1	2

3 NUMERICAL SIMULATIONS

3.1 Description of the numerical model

Buckling curves are simulated using geometrically and materially non-linear analyses with imperfections (GMNIA). 10 beam elements along the column's length are used and validated based on a mesh sensitivity study. Before the non-linear analysis, a linear bifurcation analysis (LBA) is performed to get the first instability mode shape. This mode shape is introduced as a geometrical imperfection and amplified by L/1000 as buckling curves were derived based on this value and as commonly recommended in many studies (4,33,35–37). Regarding the residual stress patterns, the preconized distribution for hot-rolled sections from ECCS (33,35,36) is implemented in the model, with peak stresses of 0.3*235=70.5MPa, as recommended for sections with *h/b*>1.2 in new standard prEN1993-1-14 (38). This ECCS residual stress model is commonly used for wide flange hot-rolled sections whatever the yield strength and the distribution is supposed to be constant over the thickness. The assumed material model is linear elastic – perfectly plastic material model without strain hardening. However, a nominal plateau slope of E/10000 has been applied for numerical stability reasons. The impact of strain hardening for relative slenderness higher than 0.2 is neglectable as failure mode is a flexural buckling instability mode; this was already assumed in another research (33,37). The assumptions behind the numerical models are summarized in *Fig. 2*.

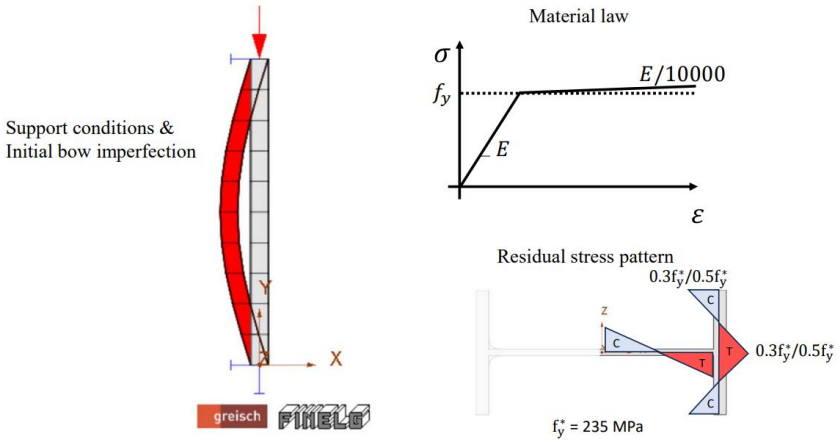

Fig. 2: Description of model assumptions for beam finite element modelling.

3.2 Validation on grades already covered in Eurocodes

To validate the accuracy of the developed numerical model, a comparison between numerical and experimental data has been carried out. The validation was performed on the experimental tests carried out at the Fritz Engineering Laboratory in 1972 (39). This campaign was an extension of the ECCS program (2) targeting heavy shape cross-sections (thickness greater than 30mm) with a height-to-width ratio higher than 1.2 which are covered in this study. The test program consists of buckling tests of pinned-end HEM340 columns for two different slenderness ratios ($L/i_z = 50$ and $L/i_z = 95$) and provides additional measurements (coupon tests, residual stress distribution, out-of-straightness). It has been decided to simulate numerically one test of both slenderness to ensure the accuracy of the numerical model to simulate buckling curves; the results are represented in Fig. 3. The linear elastic material law has been used to reproduce these experimental tests to show its relevance for such simulations.

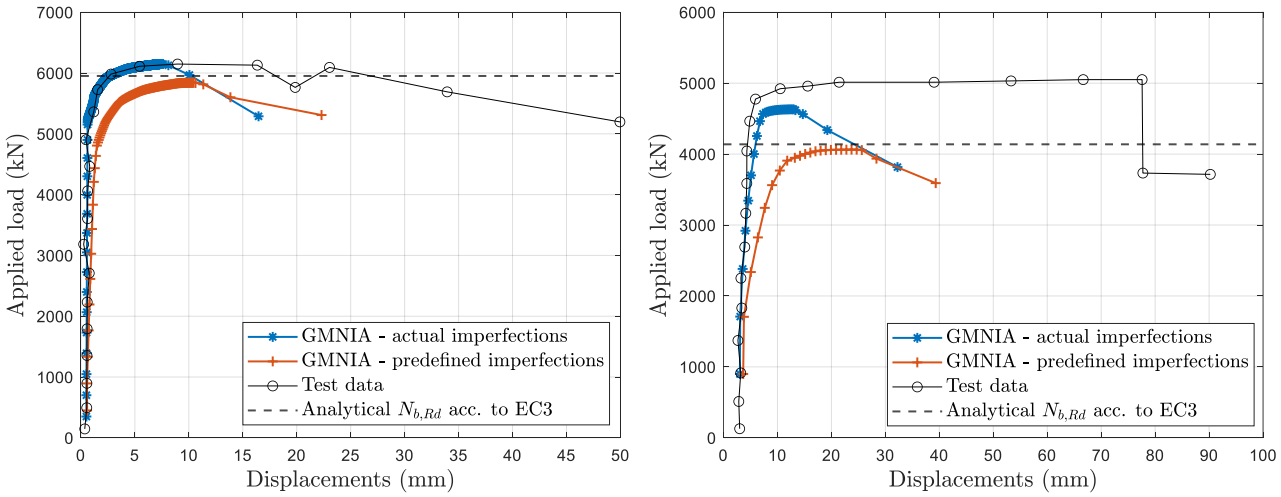

(a) Test B-1-B-2-4 (HEM340, Lcr=3.95m) (b) Test B-1-B-2-1 (HEM340, Lcr=7.5m)

Fig. 3. Validation of the numerical model based on experimental results.

As shown in Fig. 3, the numerical model provides satisfactory predictions. It should be noticed that, for test B-1-B-2-1, the numerical response is highly dependent on the residual stress pattern as the relative slenderness for this column length is close to 1.0. It is important to mention that residual stress measurements are not provided for Test B-1-B-2-1, thus the same residual stress pattern as for Test B-1-B-2-4 has been introduced leading to the observed difference in terms of peak loads. In addition, as reported in Fig. 3, other numerical simulations have been performed by considering predefined imperfections, i.e., the ECCS residual stress model and a geometrical imperfection of L/1000 to illustrate the correspondence between numerical simulations and Eurocode predictions.
The buckling curve recommendations from the current and the new upcoming versions of EN1993-1-1 (1,10) are reported in *Table 4* for the profile category under concern.

Table 4. Eurocode selection of buckling curves for flexural buckling according to (1,10)

Limits	Buckling about axis	EN1993-1-1:2005		FprEN1993-1-1:2022	
		S235-S275-S355-S420	*S460*	*S235-S275-S355-S420*	*S460 up to S700*
h/b > 1.2 / $t_f \leq$40mm	y-y	a	a_0	a	a_0
	z-z	b	a_0	b	a

As can be seen in *Table 4*, the current buckling curve for the weak axis was a bit optimistic and recent research has demonstrated that it was not appropriate (36,40,41); one lower buckling curve was seen as more suitable and the modification has been introduced in the new upcoming version FprEN1993-

1-1 (10). Therefore, the proposal in 1976, where one higher buckling curve was recommended for the high-strength steel grades, is again of application in FprEN1993-1-1 (10). Before going further in the study, numerical simulations for the two grades covered in standards, i.e. S235 and S460, were performed for the sake of validation of the above-mentioned recent research. The results are represented in *Fig. 4*.

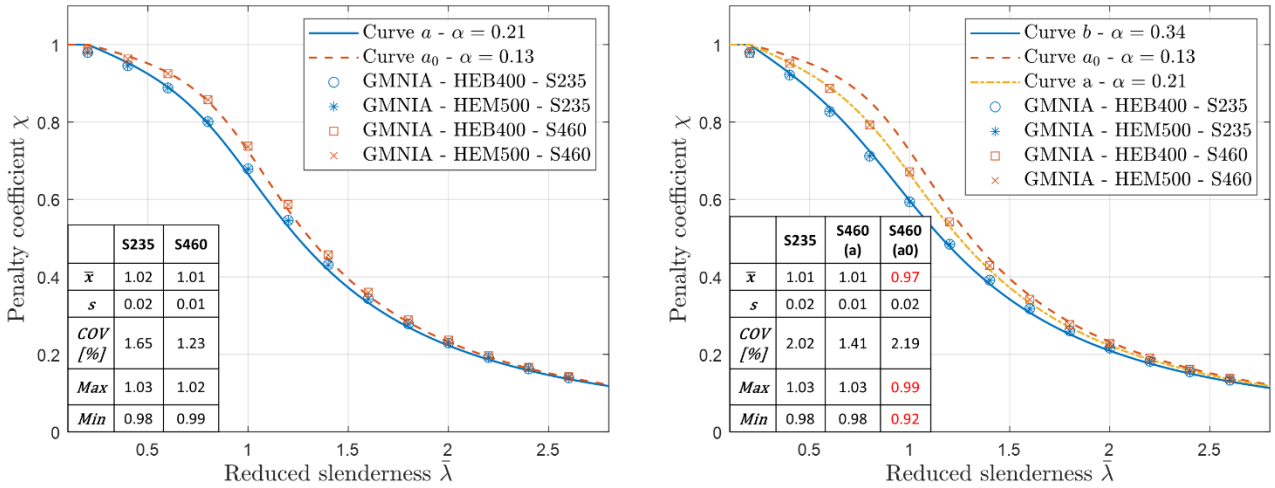

	S235	S460
$\bar{x}$	1.02	1.01
s	0.02	0.01
COV [%]	1.65	1.23
Max	1.03	1.02
Min	0.98	0.99

	S235	S460 (a)	S460 (a0)
$\bar{x}$	1.01	1.01	0.97
s	0.02	0.01	0.02
COV [%]	2.02	1.41	2.19
Max	1.03	1.03	0.99
Min	0.98	0.98	0.92

(a) h/b > 1.2 / $t_f \leq 40$mm / major axis (b) h/b > 1.2 / $t_f \leq 40$mm / minor axis

Fig. 4. Comparison between numerical simulations and Eurocode recommendations for S235 and S460.

According to *Fig. 4*, there is a good correspondence between the new upcoming Eurocode recommendations and the numerical simulations. The buckling resistance highly depends on the residual stress distributions, the geometrical imperfections, and the yield strength whereas the cross-section geometries have a negligible impact. This observation has been validated through other simulations and confirms the methodology to consider only a limited number of profiles for this study. Numerical simulations for relative slenderness of 0.2 present a reduction factor $\chi < 1.0$, meaning that, for this boundary limit between stocky and slender columns, flexural buckling appears earlier than the yielding of the cross-section. This observation is in line with other research works pointing out a lower reduction factor for this boundary slenderness (13,21). In the framework of this research, some simulations with a trilinear material law to account for strain hardening have been realized and the same peak loads were observed. Nevertheless, for the sake of continuity with existing recommendations, it has been decided to keep the length of the plateau as it is currently suggested in Eurocode 3.

3.3 Establishment of a new imperfection factor form

As a reminder, the idea is to propose a continuous imperfection factor, but strictly respecting the current recommendations for these two steel grades. The study consists of evaluating for which α the buckling curve fits with the GMNIA results (corresponding to a mean value $\bar{x}$ of 1.0 as defined in the methodology) considering a continuous vector of $\alpha \in [0.1 : 0.001 : 0.49]$. *Fig.* 5 illustrates the evolution of the calculated imperfection factor as a function of the yield strength and the proposed modified imperfection factor for the sake of comparison. In addition, results considering the minimum yield strengths prescribed in EN10025-2 and EN10025-4 (31,32) for HEM500 for which the thickness of the constitutive parts implies a yield stress reduction (see the strength reduction in *Fig.* 1) are also reported to evaluate the impact of this reduction on the results. For other cross-sections, the yield strength prescribed in *Table* 5.1 of FprEN1993-1-1 (10) is considered.

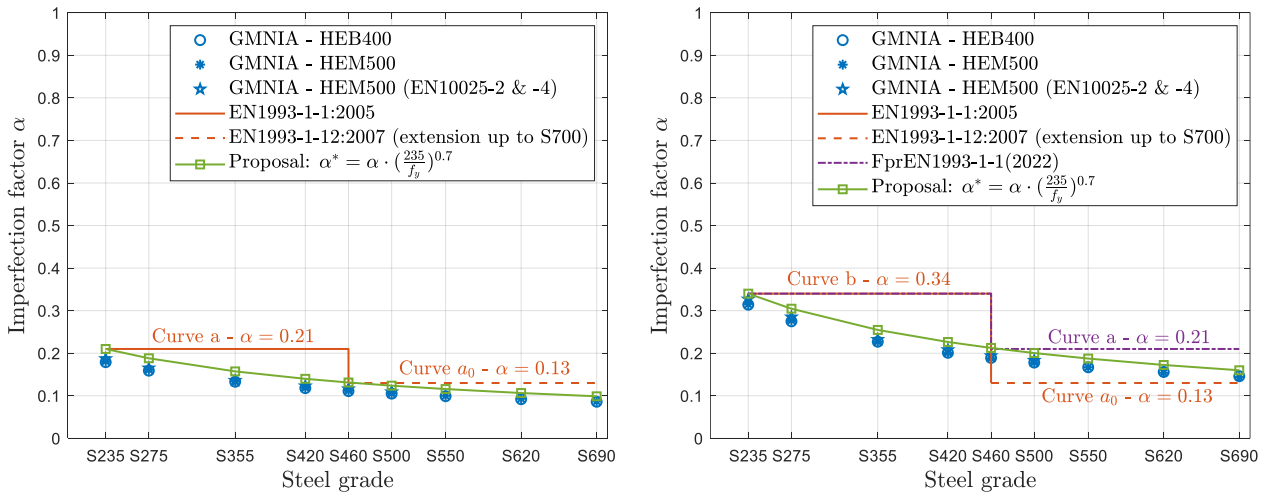

(a) h/b > 1.2 / $t_f \leq 40$mm / major axis (b) h/b > 1.2 / $t_f \leq 40$mm / minor axis

Fig. 5. Evolution of the imperfection factor α as function of the yield strength.

Fig. 5 demonstrates the negligible impact of the yield strength reduction up to flange thicknesses of 40mm; this is in line with the recommendations of FprEN1993-1-1(10) consisting of keeping the nominal yield strengths up to 40mm. *Fig*. 5 also confirms the adequacy of the proposed modification for the imperfection factor, i.e., the Maquoi's formulation (9) with an exponent of 0.7. Indeed, it gives a good correlation with numerical simulations.

4 DISCUSSIONS AND CONCLUSIONS

The review of the literature revealed that different authors already suggested the use of a continuous expression for the imperfection factor to ensure a continuity of current design rules. Comparisons based on the mean value of the ratios of the buckling reduction factors from the proposed modification presented in this paper and other modified imperfection factors proposed in the literature, i.e., the average values $\bar{x}$ of $\frac{\chi_{GMNIA}}{\chi_{EC3}}$, $\frac{\chi_{GMNIA}}{\chi_{prEN}}$, $\frac{\chi_{GMNIA}}{\chi_{Maquoi}}$ *and* $\frac{\chi_{GMNIA}}{\chi_{Jönsson}}$ are reported in *Fig. 6*.

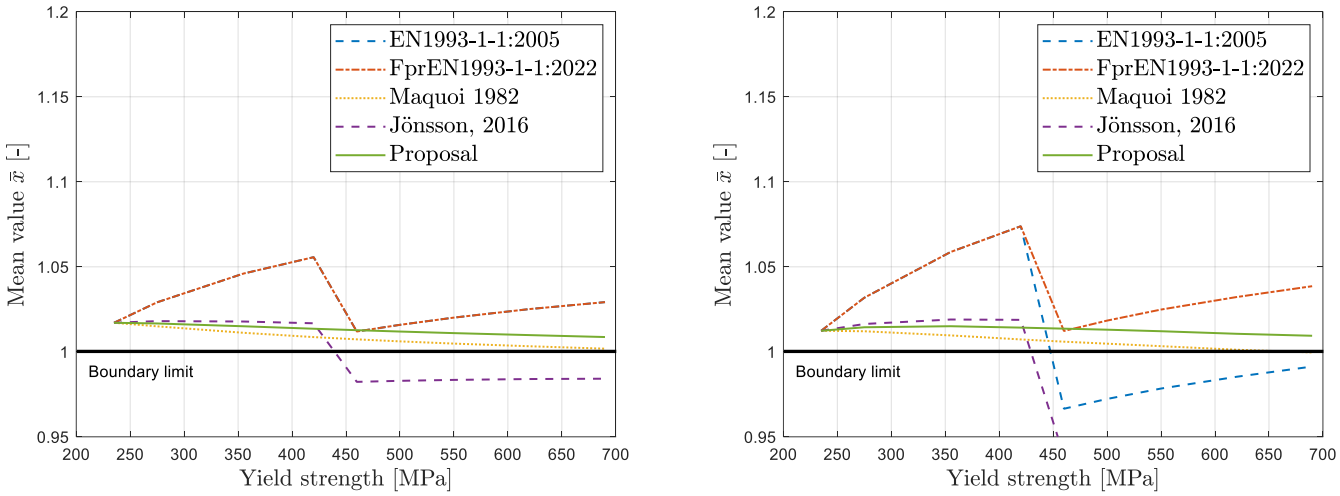

(a) h/b > 1.2 / $t_f \leq 40$mm / major axis (b) h/b > 1.2 / $t_f \leq 40$mm / minor axis

Fig. 6. Evolution of the mean values depending on the imperfection factor.

Current and future upcoming versions of Eurocode recommendations provide valid design recommendations for S235 and S460 but completely neglect the beneficial impact of yield strength

for intermediary grades and future emerging grades (yield strengths higher than 460MPa). Finally, the benefits in terms of member buckling loads resulting from the use of the proposed modified imperfection factor instead of new upcoming Eurocode recommendations are represented in *Fig. 7.*

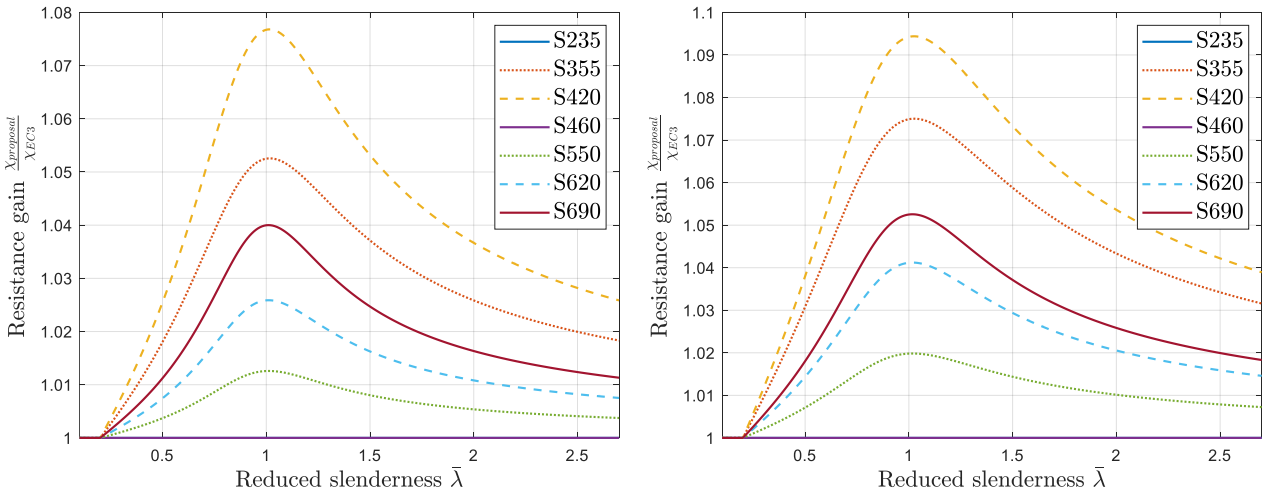

(a) Curve a (b) Curve b

Fig. 7. Resulting gains from the use of the modified imperfection factor instead of new upcoming Eurocode recommendations (10).

Fig. 7 reports significant resistance increases especially for grades S355 and S420 for which the flexural buckling resistances are currently underestimated in the Eurocode. The peak increase corresponds to a non-dimensional slenderness of 1.0, for which the residual stress distribution highly affects the results. However, even a small increase in the buckling resistance may lead to a gain of one profile, and thus to a significant reduction of the structure weight. Moreover, this modification contributes to the improvement of existing design rules, avoiding a non-physically justified stepwise evaluation of the buckling resistance when yield stress increases, and consequently, it contributes to the global objective of reducing the use of materials in future steel structures. The use of higher steel grades could also lead to cost and carbon footprint savings depending on their corresponding relative price and carbon footprint (42,43).

The proposal is validated on a well-defined profile category, i.e., profiles with $h/b>1.2$ and flange thicknesses $t_f \leq 40$mm. The validity of the modified imperfection factor proposal should be assessed on other limitations of geometrical properties; these investigations are currently ongoing at the University of Liège. In addition, Monte-Carlo simulations may be carried out to consider the variability of geometrical and material properties. Experimental column tests would also make it possible to carry out a statistical study and set the associated partial safety coefficient γ_{M1} according to annex D of EN 1990, especially tests on grades equal to or higher than 500 MPa which could appear in the upcoming years to validate the proposed trend. Finally, existing modified imperfection factors for hollow sections or welded I-beams should be analysed to investigate the possibility of having the same expression of the imperfection factor whatever the section typology.

REFERENCES

1. CEN. EN1993-1-1:2005: Eurocode 3: Design of steel structures - Part 1-1: General rules and rules for buildings. Brussels; 2005.
2. Sfintesco D. Fondement expérimental des courbes européennes de flambement. Construction métallique. 1970;3:5–12.
3. Beer H, Schulz G. Bases théoriques des courbes européennes de flambement. Construction Métallique. 1970;3(485):37–57.

4. Strating J, Vos H. Computer Simulation of the ECCS Buckling Curve using a Monte-Carlo Method. In: Construction Métallique. 1973. p. 23–39.
5. Maquoi R, Rondal J. Mise en équation des nouvelles courbes européennes de flambement. 1978;
6. Fukumoto Y, Itoh Y. Evaluation of multiple column curves using the experimental data-base approach. J Constr Steel Res. 1983;3(3):2–19.
7. Lee CH, Han KH, Uang CM, Kim DK, Park CH, Kim JH. Flexural strength and rotation capacity of I-shaped beams fabricated from 800-MPa steel. Journal of Structural Engineering. 2013;139(6):1043–58.
8. ECCS. Manual on stability of steel structures. 1976.
9. Maquoi R. Some improvements to the buckling design of centrally loaded columns. In: Structural Stability Research Council, Proceedings of the Annual Meeting. 1982.
10. CEN. FprEN1993-1-1:2022: Eurocode 3: Design of steel structures - Part 1-1: General rules and rules for buildings. Brussels ; 2022.
11. Maquoi R, Jaspart JP. Quelques réflexions à propos des courbes de flambement et de l'amplitude relative d'imperfection géométrique équivalente. Liège; 2016 Dec.
12. Sedlacek G. Buckling behaviour of hot-formed SHS in high strength steel grade E-460. Comité international pour le développement et l'étude de la construction tubulaire. 1999.
13. Meng X, Gardner L. Behavior and design of normal-and high-strength steel SHS and RHS columns. Journal of Structural Engineering. 2020;146(11):4020227.
14. Wang J, Gardner L. Flexural buckling of hot-finished high-strength steel SHS and RHS columns. Journal of Structural Engineering. 2017;143(6):4017028.
15. Rasmussen KJR, Hancock GJ. Tests of high strength steel columns. J Constr Steel Res. 1995;34(1):27–52.
16. Ma TY, Liu X, Hu YF, Chung KF, Li GQ. Structural behaviour of slender columns of high strength S690 steel welded H-sections under compression. Eng Struct. 2018;157:75–85.
17. Li TJ, Li GQ, Chan SL, Wang YB. Behavior of Q690 high-strength steel columns: Part 1: Experimental investigation. J Constr Steel Res. 2016;123:18–30.
18. Sabau G, Lagerqvist O, Baddoo N. Statistical Analysis of Flexural-Buckling-Resistance Models for High-Strength Steel Columns. Journal of Structural Engineering. 2020;146(2):4019210.
19. Shi G, Ban H, Bijlaard FSK. Tests and numerical study of ultra-high strength steel columns with end restraints. J Constr Steel Res. 2012;70:236–47.
20. Ban H, Shi G, Shi Y, Wang Y. Overall buckling behavior of 460 MPa high strength steel columns: Experimental investigation and design method. J Constr Steel Res. 2012;74:140–50.
21. Jönsson J, Stan TC. European column buckling curves and finite element modelling including high strength steels. J Constr Steel Res. 2017;128:136–51.
22. Somodi B, Kövesdi B. Flexural buckling resistance of welded HSS box section members. Thin-Walled Structures. 2017;119:266–81.
23. Somodi B, Kövesdi B. Flexural buckling resistance of cold-formed HSS hollow section members. J Constr Steel Res. 2017;128:179–92.
24. Greisch office, University of Liège. FineLg: non-linear finite element analysis program: user's manual. Liège; 2018.
25. de Goyet V. L'analyse statique non linéaire par la méthode des éléments finis des structures spatiales formées de poutres à section non symétrique. Université de Liège. 1989;
26. Boissonnade N, Degée H, Naumes J, Oppe M. Experimental and numerical investigations for I-girders in bending and shear stiffened by trapezoidal stiffeners. Advanced Steel Construction. 2008;4(1):1–12.
27. Boissonnade N, Somja H. Influence of imperfections in FEM modeling of lateral torsional buckling. In: Proceedings of the Annual Stability Conference. 2012. p. 18–21.
28. Bezas MZ, Demonceau JF, Vayas I, Jaspart JP. Experimental and numerical investigations on large angle high strength steel columns. Thin-Walled Structures 2021;159:107287.
29. Bezas MZ, Demonceau JF, Vayas I, Jaspart JP. Design rules for equal-leg angle members subjected to compression and bending. J Constr Steel Res. 2022;189:107092.
30. ArcelorMittal. HISTAR® : Innovative high strength steels for economical steel structures [Internet]. https://sections.arcelormittal.com/repository2/Sections/5_3_1_HISTAR_web.pdf
31. NBN. EN10025-2:2019: Hot-rolled products of structural steels, part 2: Technical delivery conditions for non-alloy structural steels. Brussels; 2019.

32. NBN. EN10025-4:2019: Hot-rolled products of structural steels, part 4: Technical delivery conditions for thermomechanical rolled weldable fine grain structural steels. Brussels; 2019.
33. Snijder HH, Cajot LG, Popa N, Spoorenberg RC. Buckling curves for heavy wide flange steel columns. Romanian Journal of Technical Science: Applied Mechanics. 2014;59(1/2):178–204.
34. Mathworks. MATLAB version R2019b. Natick, Massachusetts; 2019.
35. Young BW. Residual stresses in hot-rolled sections. University of Cambridge; 1971.
36. da Silva LS, Tankova T, Marques L, Rebelo C. Safety assessment of Eurocode 3 stability design rules for the flexural buckling of columns. Advanced Steel Construction–an International Journal. 2016;12(3):328–58.
37. Tankova T, da Silva LS, Rodrigues F. Buckling curve selection for HSS welded I-section members. Thin-Walled Structures. 2022;177:109430.
38. CEN. prEN1993-1-14: Eurocode 3: Design of steel structures — Part 1-14: Design assisted by finite element analysis. Brussels; 2021 Jan.
39. Tebedge N, Chen WF, Tall L. Experimental studies on column strength of European heavy shapes. Fritz Engineering Laboratory Report No. 351.7. 1972 Nov.
40. Lindner J, da Silva L. Classification of rolled I-Profiles fabricated in steel grade S460 within Table 6.2 of EN 1993-1-1. 2015;
41. Snijder HH. Recent developments regarding the next version of Eurocode 3 part 1-1 on steel structures. ce/papers. 2017;1(4):515–38.
42. Saufnay L, Demonceau JF. Establishment of reliable relative price predictions for high-strength steel members. Steel Construction. https://doi.org/10.1002/stco.202300013
43. Saufnay L, Demonceau JF. Economic and environmental assessment of high-strength steel grades. ce/papers. 2023;6(3–4):527–32.